*Solar-Terrestrial Physics. 2026, vol. 12, iss. 2, pp. 43–48. DOI: 10.12737/stp-122202605. © 2026 S.A. Kolesnik, A.N. Borisevich Published by INFRA-M Academic Publishing House*

DOI: 10.12737/stp-122202605
EDN: EMNXMX

Received September 25, 2025
Accepted December 22, 2025

# SEASONAL VARIATIONS IN DAILY MAXIMUM OF ELECTRON DENSITY IN THE F2 IONOSPHERIC LAYER DEPENDING ON SOLAR ACTIVITY ACCORDING TO THE TOMSK IONOSPHERIC STATION DATA

**S.A. Kolesnik**
*Tomsk State University,*
*Tomsk, Russia, serkol@mail.tsu.ru*

**A.N. Borisevich**
*Federal Research Center "Krasnoyarsk Science Center SB RAS",*
*Krasnoyarsk, Russia, aborisevich77@gmail.com*

**Abstract.** The paper analyzes variations in the maximum electron density of the F2 ionospheric layer ($N_m$F2), using data from the Tomsk ionospheric station for the period from 1947 to 2024, including seven 11-year solar cycles, with the aim of identifying seasonal changes in daily $N_m$F2 maxima in the mid-latitude ionosphere and their relationship with solar activity. Seasonal-daily variations of $N_m$F2 were constructed separately for low and high solar activity levels. Linear and quadratic models of the regression dependence of the $N_m$F2 daily values on the *F*10.7 index are calculated for each month of the year. Regression models are computed for both monthly medians and daily data. Quantitative comparisons and resistance factors of different models for different types of data aggregation are given.

**Keywords:** solar activity, F2 layer, regression models.

## INTRODUCTION

In the 1980s, global climate changes became a very popular topic. Model calculations based on the detected increase in greenhouse gas concentrations in the atmosphere showed changes in temperature regimes and concentrations of gas components of the mesosphere and lower thermosphere [Roble, Dickinson, 1989]. From these model calculations, an assumption was made about long-term changes in Earth's ionosphere [Rishbeth, 1990]. The first work concerning instrumental observations [Laštovička, Pancheva, 1991] dealt with the long-term dynamics of radio wave propagation parameters. It was followed by a series of papers devoted to testing the hypothesis of existence of long-term trends from long series of ionospheric measurements, starting from [Bremer, 1992]. The first Russian publication on this subject showed that trends in the critical frequency of both the E layer and the F layer have different rates in different months of the year [Givishvili, Leshchenko, 1993]. All these studies were facilitated by sufficient accumulation of data from vertical ionospheric sounding, which began on a massive scale around the world in the International Geophysical Year in 1957. By the early 1990s, many ionospheric stations had accumulated measurement series in two complete cycles of solar activity (SA). As noted in [Laštovička et al., 2006] (quoted from private correspondence with H. Rishbeth), "long-term changes can only be reliably detected during time intervals that significantly exceed the 11-year solar cycle". The problems of constructing climate trends have been discussed in detail in numerous papers over the last two decades [Laštovička, Burešova, 2023; Danilov, Konstantinova, 2020; Zherebtsov et al., 2024]. Our paper is a continuation of a series of studies [Tarashchuk, Tsybikov, 2003; Kostyukevich, Tsybikov, 2005] conducted at Tomsk State University since the early 2000s to identify trends in ionospheric parameters.

From the very beginning of ionospheric observations, it became clear that the main agent producing ionization of Earth's upper atmosphere is the solar ultraviolet radiation (UVR), which has the strongest variation associated with the 11-year SA cycle [Likhachev, 1965]. In addition to 11-year cycles, SA has longer-period variations (secular and longer), the existence of which and their effect on geomagnetism were known as early as the beginning of the XX century [Bauer, 1918]. As for description of climatic (long-term) changes in ionospheric parameters, two factors can be conditionally distinguished — global and regional. Global factors should be read as all possible effects of the Sun: variations in radiation fluxes in different ranges, the solar wind, the interplanetary magnetic field, and flare activity. Regional ones include seasonal anomalies, seasonal-diurnal variation, geomagnetic latitude and longitude features, and possible anthropogenic impact. Our main goal is to identify trends in the SA effect on the ionosphere as the major global factor. In most papers of the last thirty years, SA has been examined using regression models of plasma frequency and various SA indices [Laštovička, Burešova, 2023]. The most common SA index, by which most models of the ionosphere and upper atmosphere are parameterized, is *F*10.7.

All works dealing with long-term trends in variations of ionospheric parameters are based on statistics of time series of critical (plasma) frequency measured by ionosondes of various designs. The plasma frequency is a characteristic of the quasi-electroneutral ionosphere reflecting charged particle interactions in plasma, and the electron density is a fundamental characteristic of the ionosphere. Furthermore, in theoretical models, the ion formation rate is directly proportional to the UVR flux [Likhachev, 1965; Ivanov-Kholodnyi, Nikolskyi, 1969].

Our paper presents the results of analysis of $N_m$F2 variations from the Tomsk Ionospheric Station data for 1947–2024 including eight 11-year SA cycles in order to identify seasonal $N_m$F2 variations in the mid-latitude ionosphere and their relationship with SA.

## 1. INITIAL DATA

We use data obtained at the Tomsk Ionospheric Station (TIS, 56°49'77" N, 84°97'44" E), which has the longest and most homogeneous series of original observations from 1936 to the present.

The beginning of the analyzed series in 1947 was associated with the start of regular observations of SA in a radio frequency range, namely, with the $F$10.7 index [Tapping, 2013]. This index is expressed in solar flux units (1 s.f.u.=$10^{-22}$ W·m$^{-2}$·Hz$^{-1}$). The $F$10.7 index represents daily values. The measurements are made at local noon at the Penticton Radio Observatory (British Columbia, Canada). Measurements of the F2-layer critical frequency $f_o$F2 at TIS from 1947 to May 1957 are half-hour measurements; from June 1957, 15-min measurements. Among all the ionospheric parameters, we examine the peak electron density in the F2 layer N$_m$*F2* as a region covering most of Earth's ionosphere. To calculate $N_m$F2 from measured $f_o$F2, we used the formula

$$N_m\text{F2}\left(10^4\ \text{cm}^{-3}\right) = 1.24\, f_o\text{F2}^2\ (\text{MHz}). \qquad (1)$$

In the top panel of Figure 1, the red curve represents SA variation expressed in monthly median $F$10.7; black numerals are generally accepted numbers of solar cycles; steps denote average values for each SA cycle. Of this series of observations, cycles 21 and 22 are the most similar in shape and amplitude. The average values of $F$10.7 in these cycles coincide. In addition, the deepest and longest SA minima were recorded in the last two cycles. In 2008–2009, there were 527 days without sunspots; and in 2019–2020, 466 days. In terms of the sunspot number, these are the longest minima on record since the Maunder Minimum (1645–1715) [Liu et al., 2021]. Of course, the current SA minima are not as grand as the Maunder Minimum, but they are the lowest in the era of space exploration and more similar to the Dalton Minimum (1790–1830) [Ahluwalia, Ygbuhay, 2012].

The blue curve in the bottom panel denotes monthly medians of the daytime peak electron density. A downward linear trend (dashed line) is shown which basically corresponds to a similar trend in SA. It should be noted that in similar SA cycles 21 and 22 the ionospheric response, expressed in cycle averages of $N_m$F2, is different. In cycle 22, it is 18 % lower than in cycle 21. The differences in the response of $N_m$F2 to SA in cycles 21 and 22 may be of the same order as the feature of cycle 22 identified in [Zherebtsov et al., 2024] from ionospheric measurements in Irkutsk.

To understand the behavior of the diurnal daytime peak electron density at various SA levels, we plotted seasonal diurnal variations of $N_m$F2. Constructing models of seasonal diurnal variations can be useful for filling data gaps with interpolated values based on data obtained at other times of the day, as in [Laštovička et al., 2006]. We divide the entire range of $F$10.7 values into quarters by approximately equal numbers of them. Figure 2 presents the calculation results for the first and last quarters of SA values ($62<F10.7<78$ and $158<F10.7<325$ respectively). These quarters included ~6950 days of measurements, and averages of $N_m$F2 for each 15-min observation interval of each day of the year were calculated for them. The local time is in UT+7, and the color scale of $N_m$F2 varies for different SA levels.

The black dashed line indicates the time of navigational twilight that corresponds to a solar depression angle of 12° at the ground level or to sunset/sunrise at the height of the F2 ionospheric layer (140 km). During the summer solstice at the latitude of Tomsk at an ionospheric height >120 km, the sun shines day and night. Solid black lines denote the sunrise/sunset time in Tomsk on the Earth surface. The maroon solid line is the time of the local noon, which varies within 31 minutes throughout the year in Tomsk. The white solid line is the calculated time of daytime $N_m$F2. For different dates and SA levels, the peak is observed at 13:00–15:00 LT.

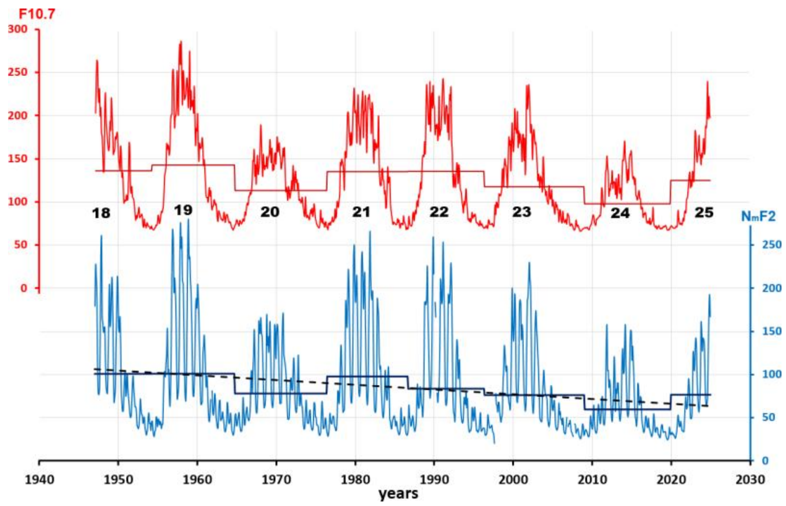


*Figure 1.* Time variations of monthly median $F$10.7 (red curve) and monthly medians of the daytime peak electron density of the F2 layer ($N_m$F2, $10^4$ cm$^{-3}$) according to data from the Tomsk Ionospheric Station (blue curve). Black numerals indicate solar cycle numbers. Steps show the average values of $F$10.7 and $N_m$F2 for each SA cycle

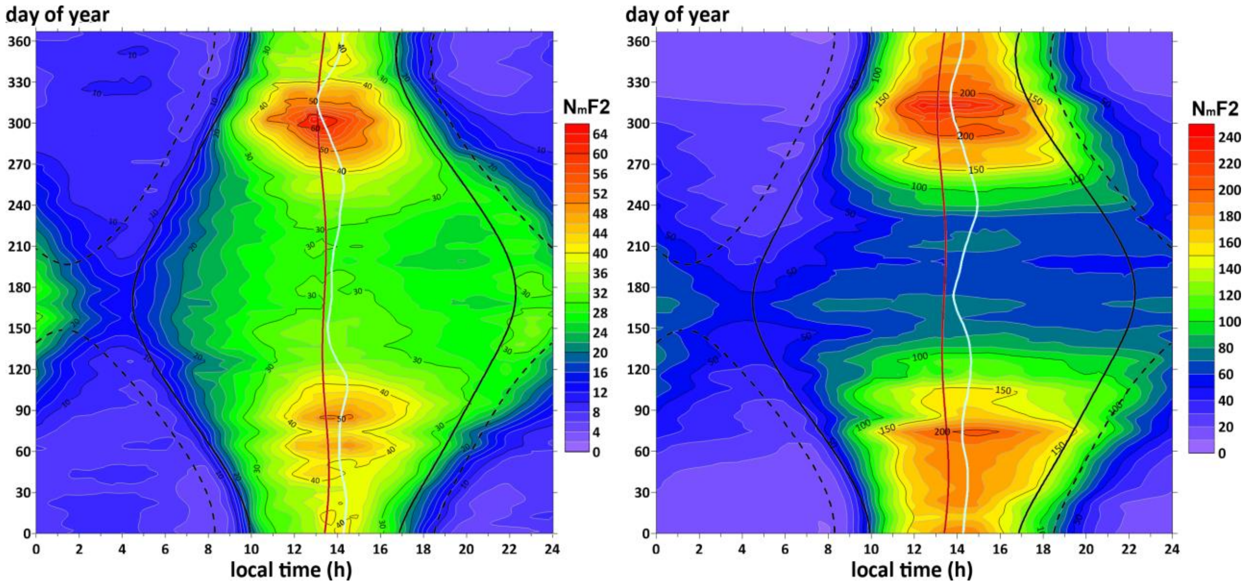


*Figure 2.* Seasonal diurnal variation of $N_m$F2 ($10^4$ cm$^{-3}$) at different SA levels: 62<$F$10.7<78 (left), 158<$F$10.7<325 (right)

At high $F$10.7, peak $N_m$F2 is on average detected 24 min later than at low $F$10.7. For December–March, the difference between the peak times at low and high SA is insignificant; for May and August, it is as large as 45 min. Thus, the daytime peak used in this work is the peak electron density calculated for each day from 13 to 15 LT.

In addition to the daytime peak, Figure 2 illustrates the occurrence of evening peak $N_m$F2 from May to August after sunset. The evening peak is most pronounced at low $F$10.7, and on some days in June and July it may be higher than the daytime peak. At high SA levels, the daytime peak is less pronounced in summer; the "flatter" behavior of the electron density is observed during daylight hours. In general, daytime peak $N_m$F2 is longer at high SA, and the electron density decreases more slowly in the evening. In absolute terms, daytime peak $N_m$F2 differs ~4 times at low and high SA. Due to seasonal and regional features of Tomsk, the maximum absolute daytime values are observed in March and November.

As for the daytime minimum $N_m$F2, from September to April it is detected along the line of navigational twilight (during sunrise at the ionospheric height of 140 km). For the same months, a secondary minimum is recorded 2 hours after sunset in the ionosphere. The bimodality of the daytime minimum is most typical for November–January at low SA.

On the basis of the obtained seasonal diurnal variations of $N_m$F2, we have selected the daytime peak observed after local noon. This parameter reflects the maximum UVR effect on the electron density of the ionosphere due to the preceding midday maximum insolation. During the year, the daytime peak in the F2 layer is observed at different times, in particular because of different time of the local noon due to Earth's elliptical orbit. For Tomsk, the maximum solar zenith angle is recorded in different months from 13:04 to 13:35 LT.

Some studies on long-term trends have been carried out using data on annual average parameters regardless of the season [Zherebtsov et al., 2024]. As a result, the correlation coefficients of annual averages of $N_m$F2 and $F$10.7 are 0.98 or higher. In view of the strongly pronounced annual, semi-annual, and seasonal variations in the mid-latitude ionosphere, it is necessary to take into account the season in order to construct regression models. Moreover, the criterion for the correct choice of regression models is the normal distribution of the residual series. In the case of linear and quadratic models without regard to the time of year, according to TIS data a bimodal distribution is observed for $F$10.7>90 (64 % of measurements). From this we can conclude that this approach is unacceptable.

## 2. EMPIRICAL DESCRIPTION

The following regressions were utilized as approximation models of the $N_m$F2 dependence on $F$10.7.

1. Linear model of electron density

$$N_m\mathrm{F2}(F10.7) = a_1 F10.7 + b_1; \quad (2)$$

2. Quadratic model of electron density

$$N_m\mathrm{F2}(F10.7) = a_2 F10.7^2 + b_2 F10.7 + c_2. \quad (3)$$

Figure 3 shows regression models of $N_m$F2 ($10^4$ cm$^{-3}$) on $F$10.7 for four months, constructed from daily and monthly median $N_m$F2 and $F$10.7. The regression coefficients for daily values calculated by the least square technique are listed in Table 1.

The quality of the regression models for each month in the form of correlation coefficients is shown in Table 2. For monthly medians of all months except June, the dependence is linear, since the correlation coefficients for the remaining months differ by no more than 1.3 %, and for June this difference is 3.9 %. As for the regression models based on daytime peaks for each observation day, the quality of quadratic models from March to October is higher than linear approximations by an average of 3.6 %.

To demonstrate the quality (form) of the $N_m$F2 dependence on $F$10.7, it is proposed to use linear filtering of

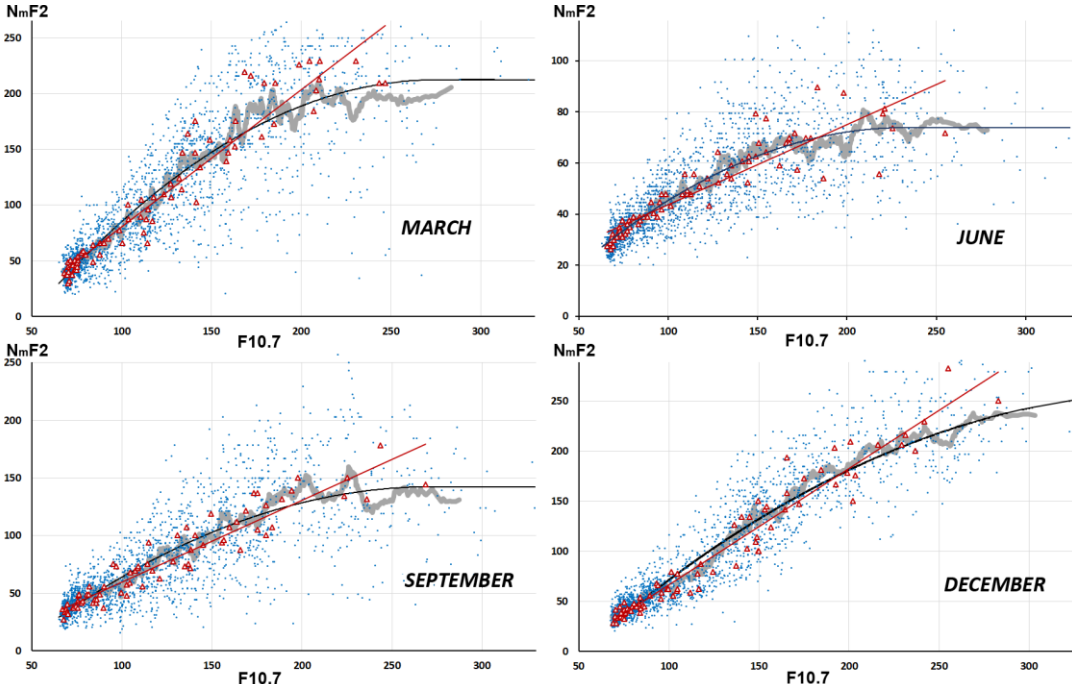


*Figure 3.* Regression models of the dependence of $N_m$F2 ($10^4$ cm$^{-3}$) on *F*10.7 for four months. Blue dots represent original daily values; the black curve, their quadratic approximation. The red curve with Δ indicates monthly medians and their linear approximation. The thick gray curve is a moving linear average over 30 regression points of daily values

Table 1

Regression coefficients of linear and quadratic approximations of $N_m$F2(*F*10.7) according to (2), (3), calculated using the least square technique

| Month | $a_1$ | $b_1$ | $a_2$ | $b_2$ | $c_2$ |
|---|---|---|---|---|---|
| January | 1.023 | –33.2 | –0.00213 | 1.698 | –77.9 |
| February | 1.096 | –35.3 | –0.00241 | 1.822 | –81.6 |
| March | 1.043 | –22.7 | –0.00412 | 2.273 | –100.9 |
| April | 0.805 | –11.9 | –0.00203 | 1.406 | –49.8 |
| May | 0.459 | 5.8 | –0.00170 | 0.964 | –26.2 |
| June | 0.276 | 16.0 | –0.00162 | 0.754 | –13,9 |
| July | 0.284 | 13.2 | –0.00178 | 0.790 | –17.8 |
| August | 0.333 | 11.6 | –0.00134 | 0.748 | –15.3 |
| September | 0.636 | –1.8 | –0.00262 | 1.431 | –52.9 |
| October | 1.017 | –14.2 | –0.00371 | 2.164 | –88.9 |
| November | 1.215 | –35.6 | –0.00256 | 1.998 | –86.1 |
| December | 1.054 | –35.4 | –0.00239 | 1.813 | –85.6 |

Table 2

Correlation coefficients between regression description and original data on $N_m$F2 by monthly median and daily peaks

| Month | Monthly medians | | Daily measurements | |
|---|---|---|---|---|
| | linear | quadratic | linear | quadratic |
| January | 0.975 | 0.975 | 0.911 | 0.921 |
| February | 0.971 | 0.971 | 0.903 | 0.911 |
| March | 0.960 | 0.967 | 0.847 | 0.874 |
| April | 0.933 | 0.939 | 0.797 | 0.809 |
| May | 0.946 | 0.945 | 0.742 | 0.765 |
| June | 0.902 | 0.937 | 0.742 | 0.785 |
| July | 0.932 | 0.945 | 0.757 | 0.800 |
| August | 0.930 | 0.937 | 0.759 | 0.784 |
| September | 0.949 | 0.955 | 0.772 | 0.797 |
| October | 0.963 | 0.973 | 0.846 | 0.870 |
| November | 0.976 | 0.976 | 0.906 | 0.914 |
| December | 0.973 | 0.974 | 0.921 | 0.932 |

successive regression values; in our case, it is a moving average over 30 points (thick gray curve). In all panels of Figure 3, there are jumps at high *F*10.7 from 150 to 250.

Figure 4 displays the obtained dependence of $N_m$F2 on *F*10.7 and season. A different quadratic approximation was used for each month of the year.

## 3. DISCUSSION

Regular extra-atmospheric satellite measurements of solar ionizing UVR began in 1977. Richards et al. [1994] describes the EUVAC model that systematizes all previous one-time rocket measurements of the solar ionizing ultraviolet spectrum and continuous satellite series of observations of individual spectral lines, which have appeared by that time. In particular, it is shown that in some spectral lines there is a linear dependence of the UVR flux on *F*10.7, which has a qualitative change at *F*10.7 =180÷225 (~200 on average). Perhaps the change which we describe by a quadratic approximation stems from the form of the dependence of the solar ionizing UVR flux on *F*10.7. The standard ionospheric model IRI [Bilitza, 2000] also uses a two-segment linear model for the dependence $N_m$F2(*F*10.7) expressed in sunspot number. The break point is set to 150. As mentioned above in the description of Figure 1, this effect cannot be studied in all SA cycles, since individual maxima of specific cycles exceed *F*10.7=150 not in all months.

Liu et al. [2021] discuss the controversy in different studies: whether there is saturation of $N_m$F2 relative to solar UVR fluxes or not. Various examples of both saturation and amplification in the behavior of this dependence for different latitudinal zones of Earth are given. As a result, it is concluded that quadratic polynomials are quite sufficient for a good description of all electron density dependences on *F*10.7.

When constructing models of the dependence of monthly median $N_m$F2(*F*10.7), *F*10.7 is limited to 250 on average (in some months, to 217–272). Monthly medians of *F*10.7>200 were observed in 9.4 % of all measurements; and *F*10.7>250±0.8 %, not every month (no more than 1 point). When using the monthly medians,

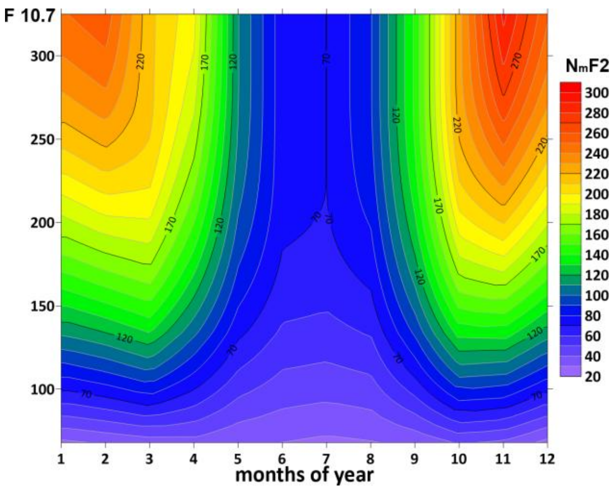


*Figure 4.* Dependence of $N_m$F2 ($10^4$ cm$^{-3}$) on *F*10.7 and season

the dynamic range of *F*10.7 of the daily baseline data used for regression models is significantly reduced (by 20–25 %). Thus, the possibility of describing the electron density behavior (qualitative and quantitative) at high *F*10.7 is lost. The consequence is that it is impossible to describe the aforementioned change reflecting the dependence of the solar UVR flux on *F*10.7. For most months, the $N_m$F2 dependence on *F*10.7 is falsely considered linear. In forecasting ionospheric parameters, it is important to have an idea about the behavior of the ionosphere over the entire range of possible *F*10.7 values. To identify the dependence of ionospheric parameters over the entire range of SA values, it is advisable to examine regression models from daily ionospheric parameters and *F*10.7, since in daily SA measurements *F*10.7>200 was observed in 10.5 % of cases; and *F*10.7>250, in 2.6 % of cases (654 measurements). Moreover, of particular interest is to find long-term trends in the electron density in individual months or seasons, since numerous studies on ionospheric climate trends discuss positive or negative trends for different stations during different observation periods in different seasons That said, the distribution of daytime peak electron density in each month is close to normal, and the calculated monthly median and monthly average $N_m$F2 values according to a number of TIS observations in 1947–2024 differ slightly, with a standard deviation ±3.8 %.

## CONCLUSION

The analysis of TIS ionospheric data has revealed seasonal diurnal variations of $N_m$F2.

For the first time, coefficients of linear and quadratic regression models have been calculated for the Tomsk region. The models describe the dependence of daytime $N_m$F2 on *F*10.7 for each month of the year for eight 11-year SA cycles. The correlation analysis has shown that it is preferable to use quadratic dependences.

For the regression models based on monthly medians, the quality of linear and quadratic models is indistinguishable, except for June, where the correlation coefficient is 3.9 % higher for the quadratic approximation. For the models based on daily values, in March–October the quality of quadratic models is by an average of 3.6 % higher than that of linear ones in correlation coefficients. The regression models based on daily values instead of monthly medians can qualitatively and quantitatively describe the electron density behavior at high SA. Thus, the dynamic range of SA values increases by 20–25 % relative to the monthly median models. Regression models have been analyzed using daily values for the first time. All the most often quoted papers of the last 25 years on this topic rely on monthly or annual resolution data.

The results can later be used to identify climatic changes in the behavior of the peak electron density or critical frequencies in the F2 layer by constructing and analyzing long-term trends.

## REFERENCES

Givishvili G.V., Leshchenko L.N. Long-term trends in the properties of mid-latitudal ionosphere and thermosphere. *Doklady of RAS* [Rep. AS Russia]. 1993, vol. 333, iss. 1, pp. 86–89. (In Russian).

Danilov A.D., Konstantinova A.V. Long-term variations in the parameters of the middle and upper atmosphere and ionosphere (review). *Geomagnetism and Aeronomy*. 2020, vol. 60, iss. 4, pp. 397–420. https://doi.org/10.1134/S0016793220040040.

Zherebtsov G.A., Ratovsky K.G., Medvedeva I.V. Long-term variations in peak electron density and temperature of mesopause region: Dependence on solar, geomagnetic, and atmospheric activities, long-term trends. *Sol.-Terr. Phys.* 2024, vol. 10, iss. 4, pp. 3–13. https://doi.org/10.12737/stp-104202401.

Ivanov-Kholodnyi G.S., Nikolskyi G.M. *The Sun and the Ionosphere. Shortwave Radiation of the Sun and its Impact on the Ionosphere.* Moscow, Nauka Publ., 1969, 455 p. (In Russian).

Kostukevich S.M., Tsibikov B.B. Long-term variations of parameters of the ionospheric F2 layer according to data from the Tomsk ionospheric station for the period 1936–2003. *Proc. VIII Young Scientists' Conference. BSHFP 2005*. Irkutsk, 2005, p. 96–97. (In Russian).

Likhachev A.I. Dependence of the ionization state at the F2 layer level on the solar wave energy influx into the Earth's atmosphere. *Doctor of Sciences Thesis.* Tomsk, 1965, 278 p. (In Russian).

Tarashchyk Yu.E., Tsibikov B.B. Long-term trends of critical frequencies according to data from ionospheric stations in Tomsk and Slow. *Bull. Tomsk State University*. 2003, no. 278, pp. 150–153. (In Russian).

Ahluwalia H.S., Ygbuhay R.C. Sunspot cycle 24 and the advent of Dalton-like Minimum. *Adv. Astron*, 2012. https://doi.org/10.1155/2012/126516.

Bauer L.A. Relation between the secular variation of the Earth's magnetism and solar activity. *Terrestrial Magnetism and Atmospheric Electricity*. 1918, vol. XXIII, no. 1.

Bilitza D. The importance of EUV indices for the international reference ionosphere. *Physics and Chemistry of the Earth (C).* 2000, vol. 25, pp. 515–521.

Bremer J. Ionospheric trends in mid-latitudes as a possible indicator of the atmospheric greenhouse effect. *J. Atmos. Solar-Terr. Phys.* 1992, vol. 54, pp.1505–1511.

Laštovička J., Pancheva D. Changes in characteristics of planetary waves at 80–100 km over Central and Southern Europe since 1980. *Adv. Space Res.* 1991, vol. 11, no. 3, pp. 31–34. https://doi.org/10.1016/0273-1177(91)90399-5.

Laštovička J., Burešová D. Relationships between $f_o$F2 and various solar activity proxies. *Space Weather.* 2023, vol. 21. https://doi.org/10.1029/2022SW003359.

Laštovička J., Mikhailov A.V., Ulich T., Elias A.G., Ortiz de Adler N., Jara V., et al. Long-term trends in foF2: A comparison of various methods. *J. Atmos. Solar-Terr. Phys.* 2006, vol. 68, iss. 17, pp. 1854–1870. https://doi.org/10.1016/j.jastp.2006.02.009.

Liu L.B., Chen Y.D., Le H.J. Response of the ionosphere to varying solar fluxes. *Upper Atmosphere Dynamics and Energetics*. *Geophysical Monograph.* 2021, pp. 301–324. https://doi.org/10.1002/9781119815631.ch16.

Richards P.G., Fennelly J.A., Torr D.G. EUVAC: A solar EUV flux model for aeronomic calculations. *J. Geophys. Res.: Space Phys.* 1994, vol. 99, № A5, pp. 8981–8992.

Rishbeth H. A greenhouse effect in the ionosphere? *Planetary and Space Sci.* 1990, vol. 38, pp. 945–948.

Roble R.G., Dickinson R.E. How will changes in carbon dioxide and methane modify the mean structure of the mesosphere and lower thermosphere? *Geophys. Res. Lett.* 1989, vol. 16, iss. 12, pp. 1441–1444. https://doi.org/10.1029/GL016i012p01441.

Tapping K.F. The 10.7 cm solar radio flux (*F*10.7). *Space Weather*. 2013, vol. 11, pp. 394–406. https://doi.org/10.1002/swe.20064.

Original Russian version: Kolesnik S.A., Borisevich A.N., published in Solnechno-zemnaya fizika. 2026, vol. 12, no. 2, pp. 47–53. https://doi.org/10.12737/szf-122202605. 

*How to cite this article*

Kolesnik S.A., Borisevich A.N. Seasonal variations in daily maximum of electron density in the F2 ionospheric layer depending on solar activity according to the Tomsk ionospheric station data. *Sol.-Terr. Phys.* 2026, vol. 12, iss. 2, pp. 43–48. https://doi.org/10.12737/stp-122202605.